Spectral Decoupling of Capacity and Entropy in Network Dynamics

Ian Todd
Coherence Dynamics
ian@coherencedynamics.com

Abstract

The distinction between geometric dimension and entropy is classical in dynamical systems theory, yet network science often implicitly conflates these axes when characterizing dynamical complexity. This tutorial paper makes the dimension-entropy distinction explicit for network dynamics via Laplacian spectral analysis. We define *spectral capacity* (slow-mode count) $C(\lambda^*)$ as the count of non-trivial Laplacian modes with eigenvalues below a threshold λ^*—a purely topological measure—and show analytically that it decouples from state entropy, which depends on noise level. The closed-form decomposition $H = 2\log\sigma + B(G)$ separates the noise contribution from the topology-dependent baseline. Simulations across canonical architectures (ring, small-world, modular, random, scale-free) validate the theory and illustrate the (C, H) phase portrait as a diagnostic tool. We provide code and figures for pedagogical use.

Keywords: network dynamics, spectral capacity, entropy, Laplacian, complexity, tutorial

1 Introduction

Complex networks exhibit rich dynamical behavior arising from the interplay of topology and local dynamics. A central question in network science is how to characterize the "complexity" of such dynamics. Two natural candidates are *dimensional capacity*—how many slow modes the topology supports—and *entropy*—how unpredictable the dynamics are. These are often conflated, with entropy used as a proxy for complexity writ large [Gómez-Gardeñes and Latora, 2008, Braunstein et al., 2006].

However, classical results in dynamical systems establish that dimension and entropy are fundamentally distinct. The correlation dimension [Grassberger and Procaccia, 1983], embedding dimension [Takens, 1981, Sauer et al., 1991], and Lyapunov dimension [Kaplan and Yorke, 1979] characterize the *geometry of the attractor*. In contrast, entropy measures characterize the *distribution over that support* [Eckmann and Ruelle, 1985]. As Eckmann and Ruelle noted, "the dimension of the attractor and its entropy are independent characteristics."

Remark 1 (Capacity vs. Dimension)**.** *The spectral capacity $C(\lambda^*)$ we define is a* mode-counting measure*—the number of slow Laplacian modes below a threshold. It is* ***not*** *a fractal dimension in the Grassberger–Procaccia sense. We use "capacity" to emphasize that this measures how many persistent degrees of freedom the topology* supports*, not the fractal structure of an attractor.*

Scope and contribution. This paper is a *tutorial synthesis* that makes the classical dimension-entropy distinction network-native. The underlying insight is not new; our contribution is:

1. A clean **spectral capacity** definition via Laplacian eigenvalue counting (Section 2);
2. A **closed-form decomposition** of state entropy into noise and topology components, yielding a rigorous decoupling proof (Section 3);
3. The (C, H) **phase portrait** as a visual diagnostic, with validated simulations and reproducible code (Section 4).

We aim for pedagogical clarity rather than claiming conceptual novelty. The value is in making an important distinction explicit and computable for network practitioners.

2 Theoretical Framework

2.1 Network Diffusion Dynamics

Consider a connected graph $G = (V, E)$ with $n = |V|$ nodes. Let L denote the normalized Laplacian:

$$L = I - D^{-1/2} A D^{-1/2} \tag{1}$$

with eigenvalues $0 = \lambda_1 \leq \lambda_2 \leq \cdots \leq \lambda_n \leq 2$.

We study linear diffusive dynamics:

$$x(t+1) = (I - \alpha L)x(t) + \eta(t) \tag{2}$$

where $\alpha \in (0, 1)$ is the diffusion rate and $\eta(t) \sim \mathcal{N}(0, \sigma^2 I)$.

In the Laplacian eigenbasis, mode k evolves as:

$$c_k(t+1) = (1 - \alpha\lambda_k)c_k(t) + \tilde{\eta}_k(t) \tag{3}$$

with relaxation time $\tau_k = 1/(\alpha\lambda_k)$. Small eigenvalues yield slow modes; large eigenvalues yield fast-decaying modes.

2.2 Spectral Capacity

Definition 2 (Spectral Capacity)**.** *The spectral capacity at threshold λ^* is:*

$$C(\lambda^*) = \left|\{k : 0 < \lambda_k < \lambda^*\}\right| \tag{4}$$

the count of non-trivial *Laplacian modes below threshold. We exclude the trivial $\lambda_1 = 0$ mode (constant eigenvector).*

This captures how many slow modes the topology supports. For $\lambda^* = 0.1$:

- **Ring lattices** have dense small-λ spectrum $\Rightarrow$ high capacity
- **Random graphs** have large spectral gap $\Rightarrow$ low capacity (often $C = 0$)
- **Modular networks** have near-degenerate community modes $\Rightarrow$ intermediate capacity

Crucially, $C(\lambda^*)$ depends *only on topology*—it is invariant to noise σ.

2.3 State Entropy Proxy

Stationarity. The trivial mode ($\lambda_1 = 0$) has eigenvalue 1 in the transition matrix $I - \alpha L$, so with additive noise it becomes a random walk rather than a stationary process. We project out this mode by centering: $\tilde{x}(t) = x(t) - \bar{x}(t)$, restricting dynamics to the $(n-1)$ nontrivial modes where stationarity holds.

Closed-form entropy. In the Laplacian eigenbasis, mode $k \geq 2$ is an AR(1) process with coefficient $a_k = 1 - \alpha\lambda_k$. Since $1 - a_k^2 = 1 - (1 - \alpha\lambda_k)^2 = \alpha\lambda_k(2 - \alpha\lambda_k)$, the stationary variance is:

$$\mathrm{Var}(c_k) = \frac{\sigma^2}{1 - a_k^2} = \frac{\sigma^2}{\alpha\lambda_k(2 - \alpha\lambda_k)} \tag{5}$$

The *state entropy proxy* H is the mean log variance over the $(n-1)$ nontrivial Laplacian modes ($k \geq 2$):

$$H = \frac{1}{n-1}\sum_{k=2}^{n} \log \mathrm{Var}(c_k) = 2\log\sigma - \frac{1}{n-1}\sum_{k=2}^{n} \log\big(\alpha\lambda_k(2 - \alpha\lambda_k)\big) \tag{6}$$

This equals $\frac{1}{n-1}\log\det\Sigma_{\perp\mathbf{1}}$, where $\Sigma_{\perp\mathbf{1}}$ is the stationary covariance restricted to the mean-zero subspace.

The decomposition is key: noise contributes an *additive shift* ($2\log\sigma$), while topology contributes a *spectrum-dependent baseline*. For fixed topology, σ moves the system along the entropy axis; across topologies, the Laplacian spectrum sets the baseline entropy at any given σ.

Remark 3 (Entropy terminology)**.** *This is* ***not*** *the entropy rate h_μ, which measures unpredictability per time step. Our proxy characterizes the* spread *of the stationary distribution—differential entropy of the state, not temporal uncertainty.*

Remark 4 (Capacity terminology)**.** *We use "spectral capacity" to mean slow-mode count, distinct from channel capacity (information theory) or flow capacity (network optimization). The term emphasizes that topology* supports *a certain number of persistent degrees of freedom.*

3 Capacity-Entropy Decoupling

Proposition 5 (Spectral Decoupling)**.** *For linear diffusion dynamics* (2) *on connected graphs with dynamics restricted to nontrivial modes:*

1. ***Iso-entropy, different capacity****: For any two graphs G_1, G_2 with different capacities $C(\lambda^*; G_1) \neq C(\lambda^*; G_2)$, there exist noise levels σ_1, σ_2 such that $H(G_1, \sigma_1) = H(G_2, \sigma_2)$.*
2. ***Fixed capacity, variable entropy****: For any fixed graph G, varying σ changes state entropy H continuously while $C(\lambda^*)$ remains constant.*

Proof. From (6), the state entropy proxy decomposes as:

$$H(G, \sigma) = 2 \log \sigma + B(G)$$

where the *baseline offset* $B(G) = -\frac{1}{n-1} \sum_{k=2}^{n} \log(\alpha\lambda_k(2 - \alpha\lambda_k))$ depends only on the Laplacian spectrum.

(1) Given two graphs with different spectra, their baseline offsets satisfy $B(G_1) \neq B(G_2)$ generically. Setting $\sigma_2 = \sigma_1 \exp\big((B(G_1) - B(G_2))/2\big)$ yields $H(G_1, \sigma_1) = H(G_2, \sigma_2)$. Meanwhile, $C(\lambda^*)$ depends only on the count of eigenvalues below λ^*, which is independent of σ.

(2) Spectral capacity $C(\lambda^*) = |\{k : 0 < \lambda_k < \lambda^*\}|$ is determined by topology alone. From the decomposition, $\partial H/\partial\sigma = 2/\sigma > 0$, so H increases monotonically with σ while $C(\lambda^*)$ remains constant. □

This makes explicit that capacity differences between topologies are *entirely determined* by their integrated eigenvalue densities $N_i(\lambda^*) = |\{k : 0 < \lambda_k^{(i)} < \lambda^*\}|$. Graph families with predictable spectral densities (e.g., d-regular graphs, stochastic block models) thus have predictable capacity scaling.

4 Results

We validate the theory on canonical architectures: ring lattices ($k = 6$ neighbors), Watts-Strogatz small-worlds, stochastic block models (4 communities), Erdős-Rényi random graphs, and Barabási-Albert scale-free networks. All have $n = 100$ nodes; $\alpha = 0.1$; $\lambda^* = 0.1$. Error bars show variation over 30 random graph realizations per topology class.

4.1 Capacity-Entropy Phase Portrait

Figure 1 shows the (C, H) phase portrait. Each topology occupies a distinct horizontal position (capacity), while noise $\sigma \in [0.5, 3.0]$ moves systems vertically (entropy). Horizontal error bars indicate capacity variability across graph realizations. Key observations:

- **Ring**: $C = 6$ (many slow modes from dense small-λ spectrum)
- **Modular**: $C = 3$ (community modes near zero)
- **Small-world**: $C = 2$ (rewiring increases spectral gap)
- **Random/Scale-free**: $C = 0$ (large spectral gap, no modes below $\lambda^* = 0.1$)

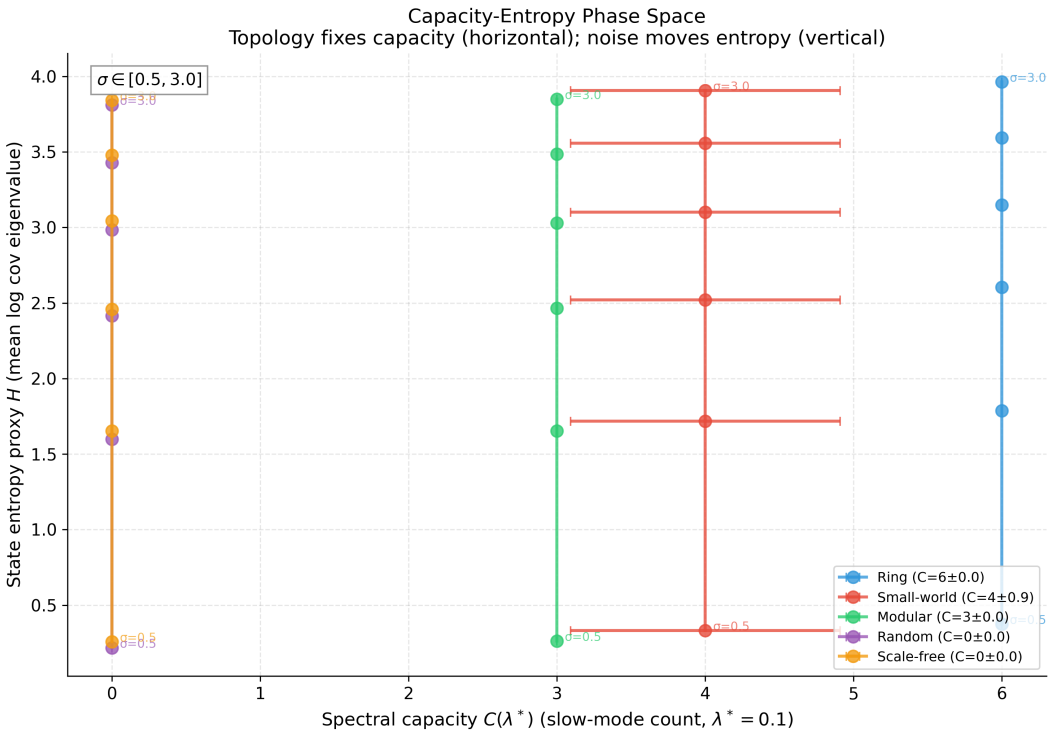

Figure 1: Capacity-entropy phase portrait. Each topology has fixed capacity (horizontal position); noise moves systems vertically along the σ range shown. Horizontal error bars show capacity variability over 30 graph realizations; entropy traces use one representative instance per topology. *Reading the portrait*: systems at the same height have equal state entropy; systems in the same column have equal capacity. Topology and noise control orthogonal axes.

4.2 Iso-Entropy Comparison

Figure 2 demonstrates Proposition 5(1). We tune σ for each topology to match state entropy at $H \approx 1.0$. Despite matched entropy: Ring has $C = 6$, Modular has $C = 3$, Random has $C = 0$.

Interpretation: If two systems have the same H but different C, they are equally "spread" in state space but differ in how many slow coordinates support persistent structure. High-capacity networks can maintain more independent slow patterns at the same overall variance.

4.3 Fixed Capacity, Variable Entropy

Figure 3 demonstrates Proposition 5(2). For a fixed modular network ($C = 3$), varying σ changes state entropy continuously while capacity remains constant.

4.4 Spectral Mechanism

Figure 4 shows the integrated density of states $N(\lambda) = |\{k : \lambda_k < \lambda\}|$ for each topology. The spectral capacity is the CDF value at threshold $\lambda^* = 0.1$ (minus the trivial mode). Ring

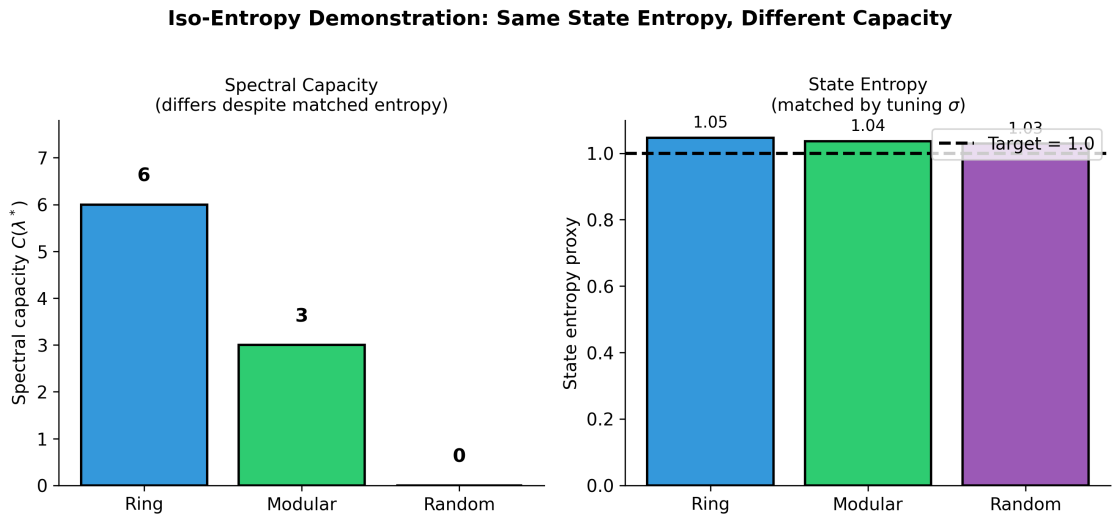

Figure 2: Iso-entropy, different capacity. Left: capacity differs substantially. Right: state entropy matched by tuning σ.

lattices have dense eigenvalues near zero; random graphs have a large spectral gap.

4.5 Threshold Sensitivity

Figure 5 shows capacity as a function of threshold λ^*. This "capacity curve" reveals how topologies separate: ring lattices accumulate capacity rapidly at small λ^*, while random graphs remain at $C = 0$ until λ^* exceeds the spectral gap ($\lambda_2 \approx 0.15$ for $n = 100$, $p = 0.15$ ER graphs).

5 Discussion

5.1 Implications

Network complexity is two-dimensional: capacity (topological) and entropy (dynamical). Entropy-only characterizations miss the capacity axis. A network can have:

- High entropy, low capacity: unpredictable dynamics in few modes (e.g., noisy random graph)
- Low entropy, high capacity: structured dynamics across many modes (e.g., coherent ring)

For **neural networks**, this distinguishes high-dimensional activity [Stringer et al., 2019] from high signal diversity [Schartner et al., 2017]. For **network design**, topology selection matters for capacity; noise tuning matters for entropy.

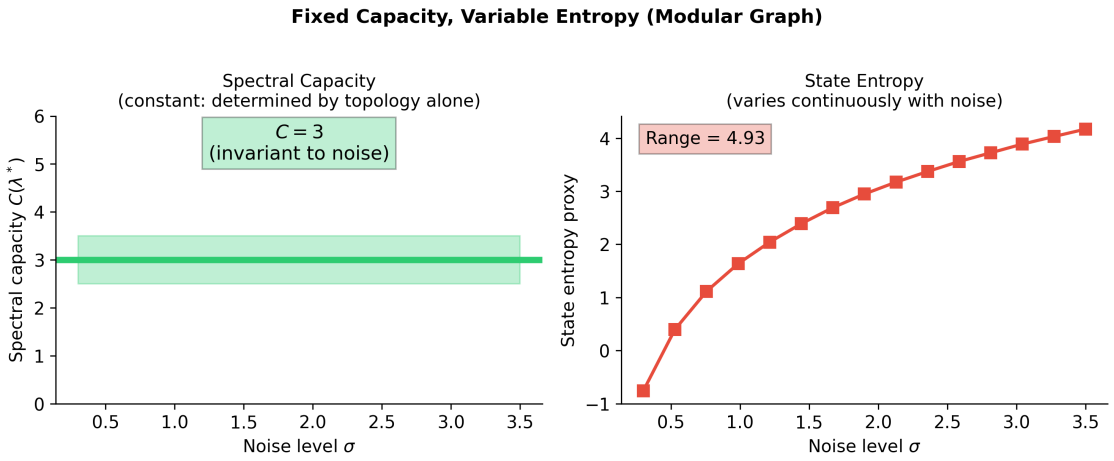

Figure 3: Fixed capacity, variable entropy. Capacity is constant (determined by topology); state entropy varies with noise.

5.2 Relation to Prior Work

The dimension-entropy distinction is classical [Eckmann and Ruelle, 1985, Grassberger and Procaccia, 1983]. This tutorial makes it network-native via Laplacian spectral analysis, but does not claim the distinction itself as novel. Related work includes entropy rate on networks [Gómez-Gardeñes and Latora, 2008], which measures temporal unpredictability rather than state spread; visibility graph correlation dimension [Lacasa and Gómez-Gardeñes, 2013]; and entrograms for community detection [Faccin et al., 2018]. The spectral gap literature [Chung, 1997] provides the mathematical foundation for our capacity definition.

5.3 Limitations

We analyzed linear diffusion; nonlinear dynamics may couple capacity and entropy in certain regimes. The threshold λ^* must be chosen appropriately—we recommend either fixing a timescale τ and setting $\lambda^* = 1/(\alpha\tau)$, or choosing λ^* as a fixed percentile of the spectrum to enable cross-network comparisons. Empirical estimation from finite data requires care.

6 Conclusion

Spectral capacity and state entropy are orthogonal axes of network complexity. Topology sets capacity through eigenvalue density; noise sets entropy. The (C, H) phase portrait provides a diagnostic for characterizing network dynamical regimes.

Data Availability

Code available at `https://github.com/todd866/spectral-decoupling`.

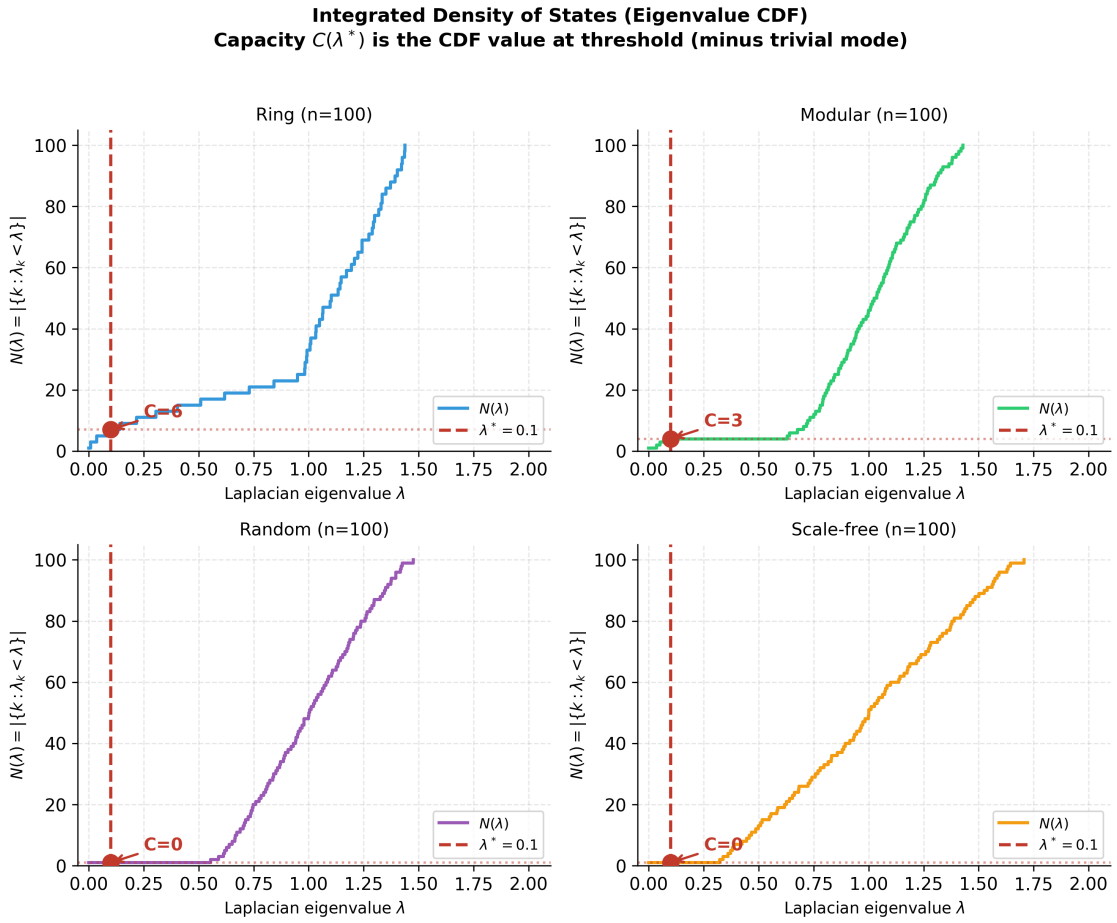

Figure 4: Integrated density of states (eigenvalue CDF). Capacity $C(\lambda^*)$ equals the CDF at threshold minus 1 (for the trivial mode). Ring has many slow modes; random has none below threshold.

References

S. L. Braunstein, S. Ghosh, and S. Severini. The Laplacian of a graph as a density matrix: a basic combinatorial approach to separability of mixed states. *Annals of Combinatorics*, 10(3):291–317, 2006. doi: 10.1007/s00026-006-0289-3.

F. R. Chung. *Spectral Graph Theory*, volume 92 of *CBMS Regional Conference Series in Mathematics*. American Mathematical Society, 1997.

J.-P. Eckmann and D. Ruelle. Ergodic theory of chaos and strange attractors. *Reviews of Modern Physics*, 57(3):617–656, 1985. doi: 10.1103/RevModPhys.57.617.

M. Faccin, M. T. Schaub, and J.-C. Delvenne. Entrograms and coarse graining of dynamics on complex networks. *Journal of Complex Networks*, 6(5):661–678, 2018. doi: 10.1093/comnet/cnx055.

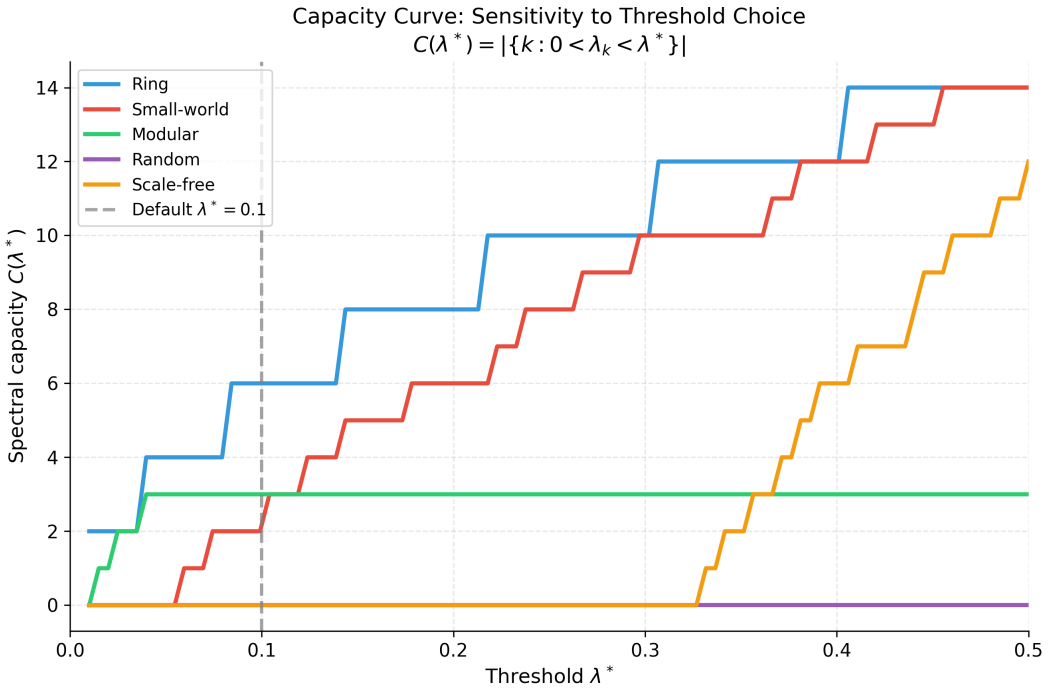

Figure 5: Capacity curve: $C(\lambda^*)$ as a function of threshold. Different topologies separate in the small-λ^* regime. Default threshold $\lambda^* = 0.1$ shown.

J. Gómez-Gardeñes and V. Latora. Entropy rate of diffusion processes on complex networks. *Physical Review E*, 78(6):065102, 2008. doi: 10.1103/PhysRevE.78.065102.

P. Grassberger and I. Procaccia. Measuring the strangeness of strange attractors. *Physica D: Nonlinear Phenomena*, 9(1-2):189–208, 1983. doi: 10.1016/0167-2789(83)90298-1.

J. L. Kaplan and J. A. Yorke. Chaotic behavior of multidimensional difference equations. *Functional Differential Equations and Approximation of Fixed Points*, pages 204–227, 1979.

L. Lacasa and J. Gómez-Gardeñes. Correlation dimension of complex networks. *Physical Review Letters*, 110(16):168703, 2013. doi: 10.1103/PhysRevLett.110.168703.

T. Sauer, J. A. Yorke, and M. Casdagli. Embedology. *Journal of Statistical Physics*, 65(3-4): 579–616, 1991. doi: 10.1007/BF01053745.

M. M. Schartner, R. L. Carhart-Harris, A. B. Barrett, A. K. Seth, and S. D. Muthukumaraswamy. Increased spontaneous MEG signal diversity for psychoactive doses of ketamine, LSD and psilocybin. *Scientific Reports*, 7(1):46421, 2017. doi: 10.1038/srep46421.

C. Stringer, M. Pachitariu, N. Steinmetz, M. Carandini, and K. D. Harris. High-dimensional geometry of population responses in visual cortex. *Nature*, 571(7765):361–365, 2019. doi: 10.1038/s41586-019-1346-5.

F. Takens. Detecting strange attractors in turbulence. In *Dynamical Systems and Turbulence, Warwick 1980*, volume 898 of *Lecture Notes in Mathematics*, pages 366–381. Springer, 1981. doi: 10.1007/BFb0091924.